Quadric Surface Fitting Applications to Approximate Dimensional Synthesis

M. John D. Hayes[*]   S. Radacina Rusu[†]
Mechanical and Aerospace Engineering,
Carleton University,
Ottawa, ON., Canada

Abstract— *An approximate synthesis method is presented that takes a given set of n desired poses of the coupler of a four-bar planar mechanism and finds the "best" mechanism that can achieve them. This is accomplished by solving an equivalent unconstrained non-linear minimization problem. The hyperboloids of one sheet or hyperbolic paraboloids that minimize the distance between the given n poses in the kinematic mapping image space and n corresponding points that belong to the quadric surfaces, represent the "best" mechanism that can achieve the desired poses. The procedure is tested successfully on an RRRR mechanism.*

Keywords: kinematic mapping; quadric surface fitting; approximate dimensional synthesis.

I. Introduction

Kinematic synthesis of planar four-bar mechanisms for rigid body guidance was first proposed by Burmester [1]. Burmester theory states that five finitely separated poses (positions and orientations) of a rigid body define a planar four-bar mechanism that can guide a rigid body exactly through those five poses. Burmester showed that the problem leads to at most four dyads that, when paired, determine at most six different four-bar mechanisms that can guide the rigid body exactly through the poses.

Although the solution to the five-pose Burmester problem yields mechanisms that have no deviation from the prescribed poses, a major disadvantage is that only five positions and associated orientations may be prescribed. The designer has no control over how the mechanism behaves for any intermediate pose. This can be a difficult challenge in confined and crowded operating spaces. To gain a measure of control over the intermediate poses it is necessary to have a means by which to synthesize a mechanism that guides a rigid body through n prescribed poses, with $n > 5$. In general, an exact solution does not exist to this problem. The problem is known as *approximate synthesis*, where the mechanism determined to be the solution will guide a rigid-body through the prescribed poses with the smallest error, typically in a least-squares sense. The approximate solution will be unique up to the error minimization criteria. The literature is rich with a large variety of numerical approaches to pure approximate kinematic synthesis of this

type, see [2], [3], [4], [5] for example.

A possibly much more intuitive approach is to build the approximation algorithm in the kinematic mapping image space introduced simultaneously, but independently in 1911 in [6] and [7]. In this paper, a novel approach to approximate kinematic synthesis for rigid body guidance is presented that uses the geometry of the image space to fit a set of points, representing desired positions and orientations, to quadric surfaces representing mechanism dyads. It is important to note that the optimization considers only kinematics. Dynamics and static force issues such as transmission angle and mechanical advantage are not considered. Such a restriction still applies to a vast array of planar four bar mechanism applications [8]. A very detailed summary of the geometry on the kinematic mapping image space can be found in [9], but a brief description of properties germane to algorithm presented in this paper is presented below.

II. Kinematic Mapping

One can consider the relative displacement of two rigid-bodies in the plane as the displacement of a Cartesian reference coordinate frame E attached to one of the bodies with respect to a Cartesian reference coordinate frame Σ attached to the other. Without loss of generality, Σ may be considered fixed with E free to move.

The homogeneous coordinates of points represented in E are given by the ratios $(x : y : z)$. Those of the same points represented in Σ are given by the ratios $(X : Y : Z)$. The position of a point $(X : Y : Z)$ in E in terms of the basis of Σ can be expressed compactly as

$$\left[\begin{array}{c} X \\ Y \\ Z \end{array}\right] = \left[\begin{array}{ccc} \cos\varphi & -\sin\varphi & a \\ \sin\varphi & \cos\varphi & b \\ 0 & 0 & 1 \end{array}\right]\left[\begin{array}{c} x \\ y \\ z \end{array}\right], \qquad (1)$$

where the pair (a, b) are the $(X/Z, Y/Z)$ Cartesian coordinates of the origin of E expressed in Σ, and φ is the orientation of E relative to Σ, respectively.

The essential idea of kinematic mapping is to map the three homogeneous coordinates of the pole of a planar displacement, in terms of (a, b, φ), to the points of a three dimensional projective image space. The image space coordinates are defined as:

[*]jhayes@mae.carleton.ca
[†]srrusu@connect.carleton.ca

$$X_1 = a\sin(\varphi/2) - b\cos(\varphi/2); \qquad X_3 = 2\sin(\varphi/2)$$
$$X_2 = a\cos(\varphi/2) + b\sin(\varphi/2); \qquad X_4 = 2\cos(\varphi/2). \quad (2)$$

The mapping is injective, not bijective: *there is at most one pre-image for each image point.* Any image point on the real line l, defined by the intersection of the coordinate planes $X_3 = X_4 = 0$, has no pre-image and therefore does not correspond to a real displacement of E. See [9], for a detailed analysis of the geometry of the image space.

To be practical, we can remove the one parameter family of image points for coupler orientations of $\varphi = \pi$, and normalize the image space coordinates by setting $X_4 = 1$. Conceptually, this implies dividing the X_i by $X_4 = 2\cos(\varphi/2)$ giving

$$X_1 = \frac{1}{2}\left(a\tan(\varphi/2) - b\right); \qquad X_3 = \tan(\varphi/2)$$
$$X_2 = \frac{1}{2}\left(a + b\tan(\varphi/2)\right); \qquad X_4 = 1. \quad (3)$$

Since each distinct displacement described by (a, b, φ) has a corresponding unique image point, the inverse mapping can be obtained from Eqs. (3): for a given point of the image space, the displacement parameters are

$$\begin{aligned} \tan(\varphi/2) &= X_3, \\ a &= 2(X_1 X_3 + X_2)/(X_3^2 + 1), \\ b &= 2(X_2 X_3 - X_1)/(X_3^2 + 1). \end{aligned} \quad (4)$$

By virtue of the relationships expressed in Eqs. (3), the transformation matrix from Eq. (1) may be expressed in terms of the homogeneous coordinates of the image space. After setting $z = 1$, which is done because no practical coupler will have a point at infinity, one obtains a linear transformation to express a displacement of E with respect to Σ in terms of the coordinates of the image point:

$$\begin{bmatrix} X \\ Y \\ Z \end{bmatrix} = \begin{bmatrix} 1 - X_3^2 & -2X_3 & 2(X_1 X_3 + X_2) \\ 2X_3 & 1 - X_3^2 & 2(X_2 X_3 - X_1) \\ 0 & 0 & X_3^2 + 1 \end{bmatrix} \begin{bmatrix} x \\ y \\ 1 \end{bmatrix}. \quad (5)$$

A. Planar Constraint Equations

Corresponding to the kinematic constraints imposed by RR- and PR-dyads are quadric constraint surfaces in the image space. A general equation is obtained when $(X : Y : Z)$ from Eqs. (5) are substituted into the general equation of a circle, the form of the most general constraint, [10]:

$$K_0(X^2 + Y^2) + 2K_1 X Z + 2K_2 Y Z + K_3 Z^2 = 0. \quad (6)$$

The result is that the constraint surfaces corresponding to RR, and PR-dyads can be represented by *one* equation (see [10], for how to include RP- and PP-dyads as well). After re-arranging in terms of the constraint surface *shape* parameters K_0, K_1, K_2, K_3, x, and y, treating the image space coordinates X_1, X_2, and X_3 as constants yields Eq. (7).

$$\begin{aligned} &\left[\tfrac{1}{4}(X_3^2 + 1)x^2 + (X_2 - X_1 X_3)x + \tfrac{1}{4}(X_3^2 + 1)y^2 - \right. \\ &\quad \left. (X_1 + X_2 X_3)y + X_2^2 + X_1^2\right] K_0 + \\ &\left[\tfrac{1}{2}(1 - X_3^2)x - X_3 y + X_1 X_3 + X_2\right] K_1 + \\ &\left[X_3 x + \tfrac{1}{2}(1 - X_3^2)y - X_1 + X_2 X_3\right] K_2 + \\ &\qquad \tfrac{1}{4}(X_3^2 + 1)K_3 = 0. \end{aligned} \quad (7)$$

For a particular dyad the associated $[K_0 : K_1 : K_2 : K_3]$, along with the design values of the coordinates of the coupler attachment point (x, y), expressed in reference frame E, are substituted into Eq. (7) revealing the image space constraint surface for the given dyad. The K_i in Eqs. (6) and (7) depend on the constraints imposed by the dyad.

For RR-dyads $K_0 = 1$ and the surface is a hyperboloid of one sheet, when projected into the hyperplane $X_4 = 1$, that intersects planes parallel to $X_3 = 0$ in circles, [11]. The K_i are termed *circular coefficients* and are defined as:

$$[K_0 : K_1 : K_2 : K_3] = [1 : -X_c : -Y_c : (K_1^2 + K_2^2 - r^2)], \quad (8)$$

where the ungrounded R-pair in an RR-dyad is constrained to move on a circle of constant radius, r, and fixed centre coordinates in Σ, (X_c, Y_c).

Linear constraints result when PR-dyads are employed. In this case $K_0 = 0$ and the constraint surface is an hyperbolic paraboloid, when projected into the hyperplane $X_4 = 1$, with one regulus ruled by skew lines that are all parallel to the plane $X_3 = 0$, [11]. The *linear coefficients* are defined as

$$[K_0 : K_1 : K_2 : K_3] = [0 : \tfrac{1}{2}L_1 : \tfrac{1}{2}L_2 : L_3], \quad (9)$$

where the L_i are line coordinates obtained by Grassmann expansion of the determinant of any two distinct points on the line, [12]. We obtain

$$\begin{aligned} &[K_0 : K_1 : K_2 : K_3] = \\ &[0 : -\tfrac{1}{2}\sin\vartheta_\Sigma : \tfrac{1}{2}\cos\vartheta_\Sigma : F_{X/\Sigma}\sin\vartheta_\Sigma - F_{Y/\Sigma}\cos\vartheta_\Sigma] \end{aligned} \quad (10)$$

where ϑ_Σ is the angle the direction of translation makes with respect to the X-axis, expressed in Σ, $F_{X/\Sigma}$, $F_{Y/\Sigma}$, represent the homogeneous coordinates $(X : Y : 1)$, expressed in reference frame Σ, of a point on the line that is fixed relative to Σ.

2

III. Fitting Displacements (Image Space Points) to Constraint Surfaces

To use kinematic mapping for approximate synthesis requires the best approximation, in a least squares sense, of the constraint surface coefficients K_0, K_1, K_2, K_3, x, and y given a suitably over constrained set of image space coordinates X_1, X_2, X_3, and X_4 which represent the desired set of positions and orientations of the coupler. The given image space points are on some space curve. The points on this curve must be projected onto the *best* fourth order curve of intersection of two constraint surfaces corresponding to two possible dyads from which a mechanism can be constructed which possesses motion characteristics *closest* to those specified. The solution to this problem *is* the solution to the approximate synthesis problem using kinematic mapping for rigid body guidance.

We may begin the search for a solution by generating a set of image space points that satisfy a known image space constraint hyperboloid. If the cardinality of the set of points is much larger than the number of constants required to define the hyperboloid then we should be able to fit the points to the surface. In other words, identify the equation, in a least squares sense, that the points satisfy.

One possibility is to identify the implicit quadric surface equations in the nullspace of the set of equations. That is, an arbitrary quadric surface has the following implicit second order equation:

$$c_0 X_4^2 + c_1 X_1^2 + c_2 X_2^2 + c_3 X_3^2 + c_4 X_1 X_2 + c_5 X_2 X_3 +$$
$$c_6 X_3 X_1 + c_7 X_1 X_4 + c_8 X_2 X_4 + c_9 X_3 X_4 = 0. \quad (11)$$

Given a sufficiently large set of points, one may be able to identify the 10 coefficients $c_0 \ldots c_9$ that define the quadric surface that is closest, in some sense, to the given points. But, two surfaces are required, one for each of the two dyads comprising the mechanism.
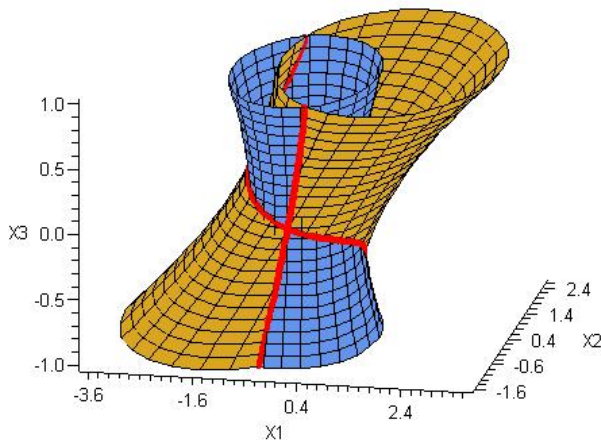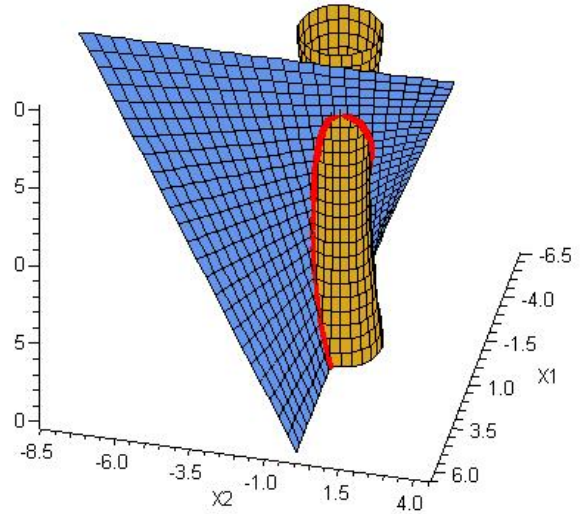

Fig. 2. Intersection curve of one RR hyperboloid of one sheet and one RP hyperbolic paraboloid.

The *best* four bar mechanism will be composed of RR, PR or RP-dyads. Due to their motion constraints, RR-dyads map to hyperboloids of one sheet, while PR and RP-dyads map to hyperbolic paraboloids in the image space [9], [11]. The two constraint surfaces that intersect in the curve closest to the reference curve will yield the best mechanism for the given set of desired poses in some sense. The curve of intersection of the quadric surfaces of the dyad pairs for $RRRR$, $RRRP$ and $PRRP$ mechanisms are illustrated in Figures 1, 2, and 3. Considering that the curve closest, in the least squares sense, to the reference curve must be the intersection of two quadric surfaces as shown above, it is obvious that the curve belongs to each of those
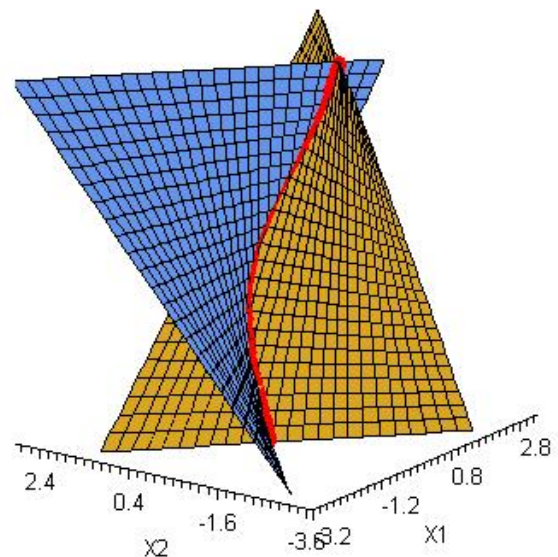

Fig. 1. Intersection curve of two RR hyperboloids of one sheet.

Fig. 3. Intersection curve of two PR hyperbolic paraboloids.

two quadric surfaces. Thus the solution to the approximate synthesis problem is finding the best two quadric surfaces (hyperboloid of one sheet or hyperbolic paraboloid) that contain a curve that is closest to the reference curve, in a least squares sense.
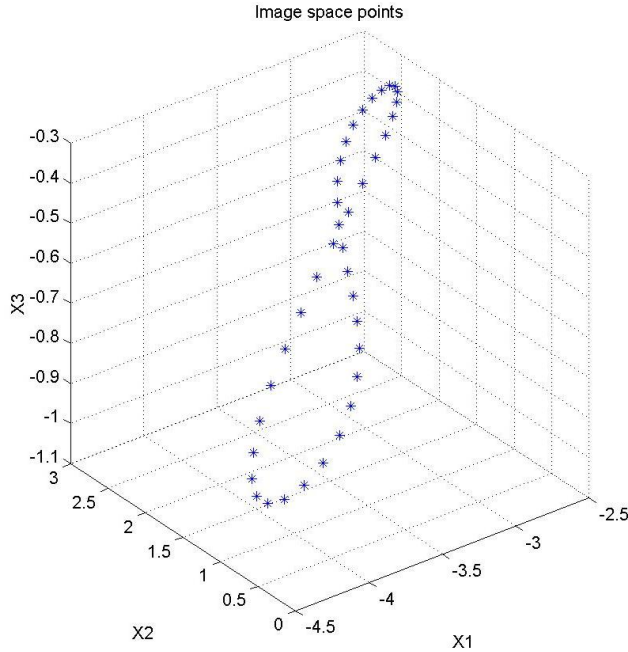

Fig. 4.   Points on 4th-order curve of intersection of two image space quadric constraint hyperboloids.
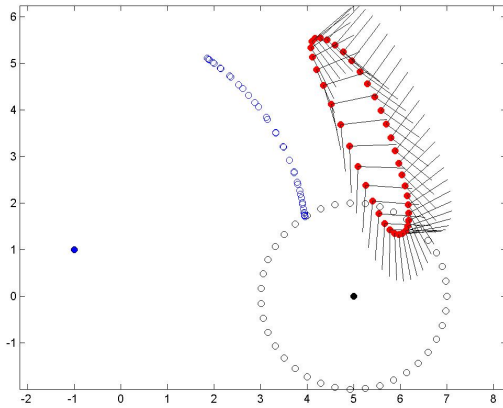

Fig. 5. The mechanism used to generate the poses.

IV. Example

The way the algorithm will be described is through an example. To generate a set of points that lie exactly on one of these constraint surfaces a parametric equation of the surface is required. It is a simple matter to parametrize Eq. (7), see [11]. Note the typo in this paper in Eq. (7):

the $-$ signs should be replaced by $+$ signs so that it reads $K_0(X^2 + Y^2) + 2K_1XZ + 2K_2YZ + K_3Z^2$. The parametrization is

$$\begin{bmatrix} X_1 \\ X_2 \\ X_3 \end{bmatrix} = \frac{1}{2} \begin{bmatrix} ([x - K_1]t + K_2 + y) + (r\sqrt{t^2+1})\cos\zeta \\ ([y - K_2]t - K_1 - x) + (r\sqrt{t^2+1})\sin\zeta \\ 2t \end{bmatrix},$$
$$\zeta \in \{0, \ldots, 2\pi\},$$
$$t \in \{-\infty, \ldots, \infty\}, \tag{12}$$

where x and y are the coordinates of the moving revolute centre expressed in the moving frame E, K_1 and K_2 are the coordinates of the fixed revolute centre expressed in Σ multiplied by -1 (i.e., $K_1 = -X_c$ and $K_2 = -Y_c$), r is the length between the moving and fixed revolute centres, while t and ζ are free parameters. To simplify the coefficients begin with the surface having the following shape parameters: $K_0 = X_4 = z = 1$, $K_1 = K_2 = x = y = 0$, $r = 2$, $K_3 = -4$ (recall that $K_3 = K_1^2 + K_2^2 - r^2$). A set of 40 image space points, shown in Figure 4 was generated by the linkage geometry, illustrated in Figure 5

Using the general quadric surface equation, Eq. (11), the image space coordinates of the 40 poses generate a set of 40 synthesis equations in terms of the 10 surface shape parameters $\{c_0, c_1, \cdots, c_9\}$. The two quadric surfaces that best fit the given points lie in the null space of the synthesis matrix $\mathbf{A}$, whose same numbered elements in each row are the terms of the $X_i, i \in \{1, 2, 3, 4\}$ scaled by the surface shape parameters, $c_i, i \in \{0, 1, \cdots, 9\}$. The two surfaces closest, in a least squares sense, to the null space of $\mathbf{A}$ can be identified using singular value decomposition (SVD). Applying SVD to the overconstrained set of synthesis equations $\mathbf{Ac} = \mathbf{0}$ reveals that the matrix $\mathbf{A}$ is rank deficient by two. That is, two of its singular values are zero, or computationally close to zero. In this case the two smallest singular values are 1.0×10^{-15}, and 3.0×10^{-15}. Hence, the two smallest singular values may be considered to be effectively zero, and near the numerical resolution of the computer. The next smallest singular value is 6.5×10^{-3}, which is five orders of magnitude smaller than the largest singular value of 88.8. It is a simple matter to identify the array of surface shape parameters, $\mathbf{c}$, that correspond to the two smallest singular values of the synthesis matrix $\mathbf{A}$ [13]. The coefficients are listed as Surfaces M, N and O in Table I, with M corresponding to the smallest, N the second smallest, and O the third smallest singular value.

The quadric surface type information is embedded in its coefficients. The implicit equation of the quadric surface can be classified according certain invariants of its discriminant and quadratic form [14]. Written in discriminant form,

Surface	c_0	c_1	c_2	c_3	c_4	c_5	c_6	c_7	c_8	c_9
M	1.0000	0.1380	0.0738	-0.3967	-0.0962	0.1201	0.0473	0.8249	-0.3372	-0.2950
N	1.0000	0.2603	0.5297	2.1392	0.0424	-0.0456	0.0145	0.7035	-1.0782	3.9373
O	1.0000	-0.3583	-0.3583	-0.0271	0.0000	-0.4448	0.1494	-0.9881	0.1732	0.0509

TABLE I. The surface shape parameters identified with SVD.

Surface	rank($\mathbf{D}$)	rank($\mathbf{Q}$)	sign of det($\mathbf{Q}$)	sign of T_1	sign of T_2	Quadric surface
M	4	3	+	+	-	Hyperboloid of one sheet
N	4	3	-	+	+	Hyperboloid of two sheets
O	3	3	+	-	+	Hyperboloid of one sheet

TABLE II. Quadric constraint surface type.

Eq. (11) becomes:

$$\begin{bmatrix} X_1 \\ X_2 \\ X_3 \\ X_4 \end{bmatrix}^T \begin{bmatrix} c_1 & \frac{1}{2}c_4 & \frac{1}{2}c_6 & \frac{1}{2}c_7 \\ \frac{1}{2}c_4 & c_2 & \frac{1}{2}c_5 & \frac{1}{2}c_8 \\ \frac{1}{2}c_6 & \frac{1}{2}c_5 & c_3 & \frac{1}{2}c_9 \\ \frac{1}{2}c_7 & \frac{1}{2}c_8 & \frac{1}{2}c_9 & c_0 \end{bmatrix} \begin{bmatrix} X_1 \\ X_2 \\ X_3 \\ X_4 \end{bmatrix} = \quad (13)$$

$$\mathbf{X^T D X}.$$

The associated quadratic form is:

$$\mathbf{Q} = \begin{bmatrix} c_1 & \frac{1}{2}c_4 & \frac{1}{2}c_6 \\ \frac{1}{2}c_4 & c_2 & \frac{1}{2}c_5 \\ \frac{1}{2}c_6 & \frac{1}{2}c_5 & c_3 \end{bmatrix}. \quad (14)$$

Both the discriminant, $\mathbf{D}$, and the quadratic form, $\mathbf{Q}$, are square symmetric matrices. It can be shown [14] that quadric surfaces can be classified by conditions on the rank of the discriminant, rank($\mathbf{D}$), the rank of the quadriatic form, rank($\mathbf{Q}$), the sign of the determinant of the discriminant, det($\mathbf{D}$), the sign of the product of det($\mathbf{Q}$) with the trace of $\mathbf{Q}$ (indicated by T_1), and the sign of the sum of the two-rowed principal minors of $\mathbf{Q}$ (indicated by T_2). This last invariant is more precisely defined as

$$T_2 = \sum_{i=1,j=2,i<j}^{3} \begin{vmatrix} q_{ii} & q_{ij} \\ q_{ij} & q_{jj} \end{vmatrix}, \quad (15)$$

where the q_{ij} are the elements of $\mathbf{Q}$.

A quadric surface is an hyperboloid of one sheet if rank($\mathbf{D}$) = 4, rank($\mathbf{Q}$) = 3, det($\mathbf{D}$) > 0, and either $T_2 \leq 0$, or both $T_1 \leq 0$ and $T_2 > 0$. A quadric surface is an hyperboloid of two sheets if all the above conditions on the invariants are met, with the exception that det($\mathbf{D}$) < 0. A quadric surface is an hyperbolic paraboloid if rank($\mathbf{D}$) = 4 and rank($\mathbf{Q}$) = 2. The values of these parameters for each of Surfaces M, N, and O are listed in Table II.

Surfaces M and O are two hyperboloids of one sheet, while Surface N is a hyperboloid of two sheets. Since a hyperboloid of two sheets does not represent a planar dyad constraint surface, the conclusion is that the quadric surfaces that best fit the reference curve, in the least squares

sense, are two hyperboloids of one sheet. Despite the fact that the second RR-dyad constraint surface is far removed from the null space of the synthesis matrix, it nevertheless indicates that an $RRRR$ mechanism will best approximate the desired coupler poses.

A. Minimization

Points on a hyperboloid of one sheet can be obtained using Eq. (12), where K_1, K_2, K_3, x, and y are the constraint surface shape parameters described in Section II-A. The approximate synthesis problem can be solved using an equivalent unconstrained non-linear minimization problem. This problem can be stated in the following way: find the set of surface shape parameters (K_1, K_2, K_3, x, y) that minimize the total spacing between all 40 points on the reference curve and 40 points that lie on the surface of a hyperboloid of one sheet where $t = X_3 = X_{3_{ref}}$:

$$d = \sum_{i=1}^{40} \sqrt{(X_{1ref_i} - X_{1_i})^2 + (X_{2ref_i} - X_{2_i})^2}. \quad (16)$$

The two sets of parameters that minimize d represent the two *best* constraint surfaces that intersect *closest* to the reference curve. Therefore, they represent the *best* dyad pair that approximate the desired 40 poses. This formulation results from the fact that $t = X_3$ is a free parameter in the parametric equation for the hyperboloid of one sheet, Eq. (12). Thus, for any hyperboloid of one sheet there exist 40 points with the same $t = X_3$ coordinates as the 40 points on the reference curve. Furthermore X_1 and X_2 have the same form in Eq. (12), so the distance between each point on the reference curve and each corresponding point on the quadric surface in the hyperplane $t = X_3$ can be simply measured on the $X_1 X_2$ hyperplane. Hence, d can be defined.

The second free parameter, ζ, in Eq. (12) is found by a minimization sub routine, which runs for each corresponding point generated on the quadric surface with the same $t = X_3$ coordinate as a point on the reference curve. This simply implies that for a constraint hyperboloid of one sheet

cut by a plane corresponding to $t = X_3$ there is only one point on the circular trace of the hyperboloid of one sheet in that hyperplane that is closest to the corresponding point on the reference curve and that the (X_1, X_2) coordinates of the closest point are only a function of ζ. Another implication is that the distance between the point generated with coordinates (X_1, X_2) and the corresponding point on the reference curve is only dependent on the surface shape parameters K_1, K_2, K_3, x, and y.

B. Initial Guesses

In order for the algorithm to converge to the solution that minimizes d, decent initial guess for the shape parameters are required. While initial guesses may be good or bad, the minimization algorithm above allows for each of them to converge to the best solution and to quantify the deviation of the poses generated by the identified mechanism. Out of the 40 points on the reference curve five points spaced relatively widely apart are arbitrarily chosen giving five equations in the five unknown surface shape parameters, after setting $K_0 = 1$ in Eq. (7), knowing that the surface should be a hyperboloid of one sheet. Seven initial guesses are tabulated in Table III.

The idea behind this technique is that the curve that is closest to the reference curve is by definition also closest to the points on the reference curve and thus a curve that exactly passes through five of the points may also be relatively close to the best curve being sought. The minimization algorithm will iteratively jump to the closest curve from curves that may be close to the reference curve by minimizing d. Furthermore, the initial guess procedure could be repeated for a different set of points on the reference curve and more initial guesses can be found. Statistics and heuristics could be used to actually narrow down the initial guesses. For the sake of testing this approximate synthesis method, this is not done, and all initial guesses are considered equal and all resulting solutions are evaluated.

C. Minimization Results

Non-linear unconstrained programming methods such as the Nelder-Mead simplex method [15] and the Hookes-Jeeves method [16] have been used with similar outcomes. The results of the minimization corresponding to each initial guess can be observed in Figures 6-12.

In each figure, the solid dots represent the desired 40 poses in the projection of the kinematic mapping image space into the hyperplane $X_4 = 1$. These 40 reference points lie on the solid reference curve. The small circles are the corresponding 40 points generated by the mechanism identified from the minimization algorithm. These points lie on the surface of a constraint hyperboloid of one sheet that the algorithm converged to starting from the particular initial guess. The results can now be visually compared. In each figure, the images on the left are the results and reference curve projected onto the plane $X_3 = 0$.
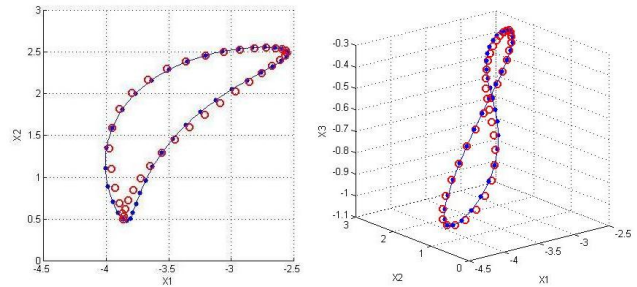

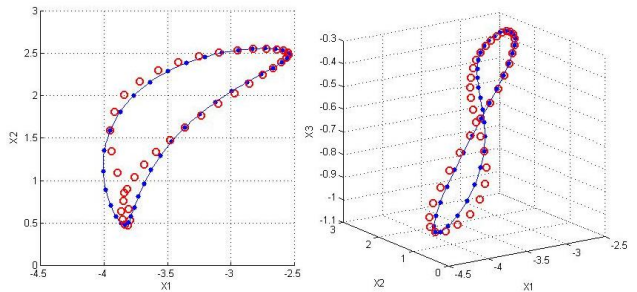Fig. 6. Graphical results for Initial Guess 1.
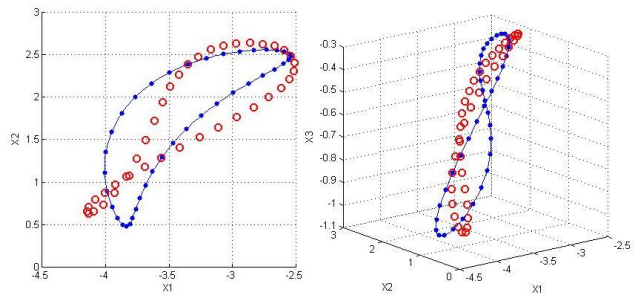

Fig. 7. Graphical results for Initial Guess 2.
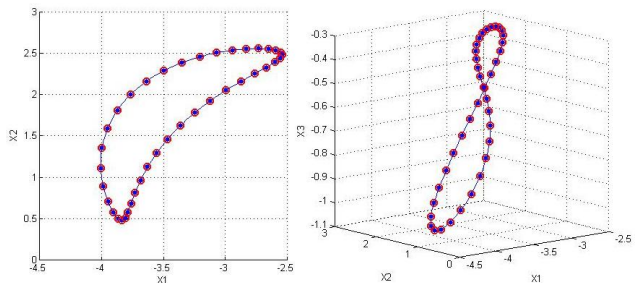

Fig. 8. Graphical results for Initial Guess 3.

Fig. 9. Graphical results for Initial Guess 4.

Guess	K_1	K_2	K_3	x	y
1	-73.59218	-21.00890	5467.99420	23.99357	56.20798
2	-7.08742	-5.53320	46.84468	-1.58544	-3.19723
3	9.75170	5.29780	27.84599	-2.29188	-7.86290
4	-5.00000	0.00000	21.00000	3.00000	-2.00000
5	1.00000	-1.00000	-23.00000	-1.00000	-2.00000
6	-20.98570	-14.15501	297.79812	-1.28879	0.56361
7	-3.05304	-6.54866	48.44514	-3.82887	-1.05131

TABLE III. Initial Guesses.

Parameter	Guess 1	Guess 2	Guess 3	Guess 4	Guess 5	Guess 6	Guess 7
K_1	-97.720	-18.202	888.914	-5.000	1.000	-25.445	-1.398
K_2	-57.463	-12.363	432.395	0.000	-1.000	-17.073	-6.191
K_3	1491.757	261.650	-2374.375	21.000	-23.000	390.531	36.554
x	-1.133	-1.287	-0.894	3.000	-1.000	-1.309	-4.388
y	0.534	0.889	-5.375	-2.000	-2.000	1.030	-2.361
Iterations	450	623	718	101	176	745	436
d	1.1132	1.9333	6.726	0.0004	0.0010	1.5746	4.8138

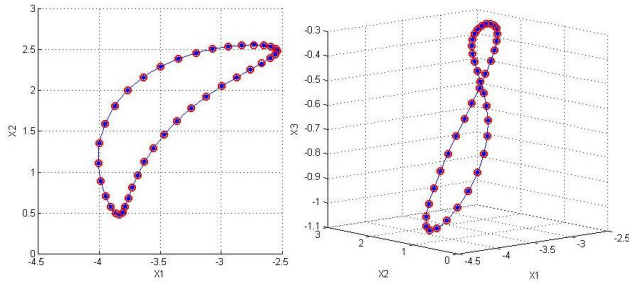TABLE IV. Results.

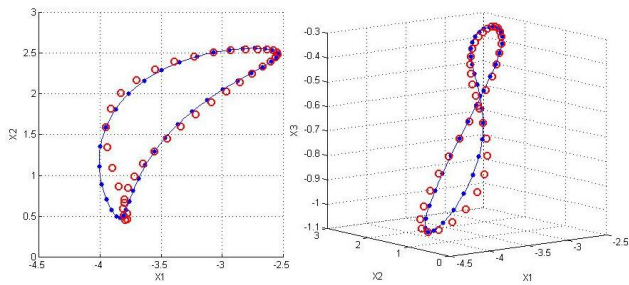Fig. 10. Graphical results for Initial Guess 5.

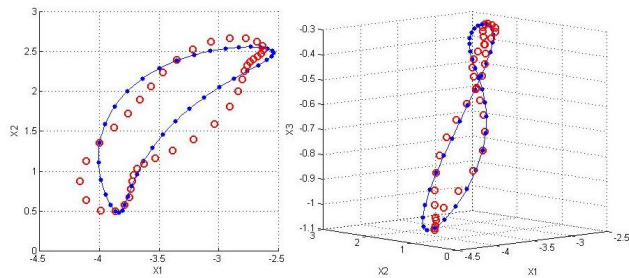Fig. 11. Graphical results for Initial Guess 6.

Fig. 12. Graphical results for Initial Guess 7.

The numerical results are tabulated in Table IV. The values of d that resulted from the minimization algorithm can now be compared. These values indicate how close the particular hyperboloid of one sheet obtained is to the reference curve. It is evident that Initial Guesses 4 and 5 generate the best hyperboloids of one sheet that intersect closest to the 40 points on the reference curve. The geometry of the best generating $RRRR$ mechanism can now be extracted using this pair of RR-dyads and their surface shape parameters.
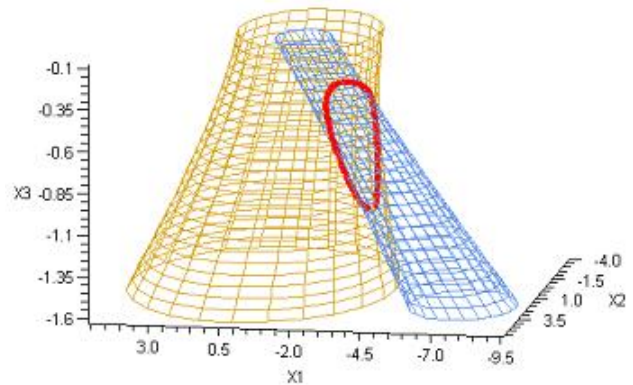

Fig. 13. Curve of intersection of *best* hyperboloids of one sheet.

It is to be noted that these are exactly the RR-dyads that were originally used to construct the initial given 40 poses, and hence the approximate synthesis was indeed successful. It should also be noted that the initial guess values for the shape parameters listed in Table III are completely different from the shape parameters that resulted from the minimization algorithm with the corresponding initial guess with the exception of Initial Guesses 4 and 5. This is not the case

for the other initial guesses because, even though the corresponding hyperboloid of one sheet fit the five arbitrarily chosen points on the reference curve well, the quadric surfaces very poorly fit the 40 points on the reference curve and the algorithm converged to a different, better solution. The curve of intersection of the best hyperboloids of one sheet corresponding to Initial Guesses 4 and 5 can be seen in Figure 13.

D. What Happens When Specified Poses are Not Perfect?

Arguably the example was contrived to be successful, but is also very illustrative of the importance of good initial guesses. The specified 40 poses lie exactly on the curve of intersection of two constraint hyperboloids of one sheet. To introduce poses that do not lie perfectly on such a 4th order curve which lies exactly on two constraint hyperboloids of one sheet, the initial specified 40 poses were truncated to 2 decimal places to introduce error, and the approximate synthesis algorithm was rerun. The results obtained are listed in Table V.

Parameter	Truncated Guess 4	Truncated Guess 4
K_1	-5.01374158	1.00543179
K_2	0.00000497	-0.99534789
K_3	21.12526403	22.98658405
x	3.00653176	-1.00047287
y	-1.98696494	-2.01010896
Iterations	134	329
d	0.1194434	0.0740493

TABLE V. Truncated Results.

It is to be seen that the fit is worse than that for the mechanism identified from the results in Table IV, still the minimization converged to similar results in terms of the best RR-dyad pair.

V. Conclusions

Kinematic mapping of distinct displacement poles to distinct points in a 3D projective image space was successfully used for approximate kinematic synthesis for rigid body guidance. A new approximate synthesis method was developed and successfully tested, and could have a wide range of applications as it has been presented in a general way which can be further expanded or simplified.

For the case of a mechanism containing a PR-dyad, the same method can be used with the exception that the conditions on the identified quadratic form of the quadric that best satisfied the specified poses will indicate that the specified image space points best fit a constraint hyperbolic paraboloid. No heuristics are necessary and given the initial desired poses, the entire approximate synthesis can be carried out using software to return a list of the best generating mechanisms ranked according to d, their *closeness*

to the given poses. The unconstrained non-linear programming problem developed has only five variables and is easily solved by several methods. A minimization algorithm could actually be further customized to "jump" from local minima to other local minima depending on the desired closeness to the given poses. Furthermore some relationships between the variables could be built in to the algorithm so it recognizes undesirable solutions from the perspective of surface shape parameters and avoids iterations in those directions.

The method developed drives the solution mechanism to achieve exactly the desired poses but not necessarily a line of best fit through the poses. This may be desirable for a mechanism designer who wants a point on the coupler to go through exactly some specified poses but does not care about the path in between them. If this is not satisfactory then the designer can simply specify more points where the path is not well defined and the approximate synthesis method will yield a more desirable solution.

References

[1] L. Burmester. *Lehrbuch der Kinematik*. Arthur Felix Verlag, Leipzig, Germany, 1888.
[2] J.E. Holte, T.R. Cahse, and A.G. Erdman. Mixed Exact-Approximate Position Synthesis of Planar Mechanisms. *ASME, J. of Mech. Des.*, 122: 278286, 2000.
[3] J. Yao and J. Angeles. Computation of All Optimum Dyads in the Approximate Synthesis of Planar Linkages for Rigid-Body Guidance. *Mechanism and Machine Theory*, 35(8): 10651078, 2000.
[4] A. Liu and T. Yang. Finding All Solutions to Unconstrained Nonlinear Optimization for Approximate Synthesis of Planar Linkages Using Continuation Method. *ASME, J. of Mech. Des.*, 121(3): 368374, 1999.
[5] X. Kong. Approximate Kinematic Synthesis of Linkages Using Generalized Inverse Matrix and Continuation. *Mechanical Science and Technology*, 18(1): 3840, 1999.
[6] W. Blaschke. Euklidische Kinematik und nichteuklidische Geometrie. *Zeit. Math. Phys.*, 60: 61-91 and 203-204, 1911.
[7] J. Grünwald. Ein Abbildungsprinzip, welches die ebene Geometrie und Kinematik mit der räumlichen Geometrie verknüpft. *Sitzber. Ak. Wiss. Wien*, 120: 677-741, 1911.
[8] A.G. Erdman, G.N. Sandor and S. Kota *Mechanism Design: Analysis and Synthesis, 4th Ed.* Prentice Hall, 2001
[9] O. Bottema and B. Roth. *Theoretical Kinematics*. Dover Publications, Inc. New York, NY, U.S.A., 1990.
[10] M.J.D. Hayes, P.J. Zsombor-Murray, and C. Chen. "Kinematic Analysis of General Planar Parallel Manipulators". *ASME, Journal of Mechanical Design*, 126(5): 866-874, 2004.
[11] M.J.D. Hayes, M.L. Husty. "On the Kinematic Constraint Surfaces of General Three-Legged Planar Robot Platforms". *Mechanism and Machine Theory*, 38(5): 379-394, 2003.
[12] M.J.D. Hayes, T. Luu, X.-W. Chang. "Kinematic Mapping Application to Approximate Type and Dimension Synthesis of Planar Mechanisms". *9th Advances in Robotic Kinematics*, eds. Lenarčič, J. and Galletti, C., Kluwer Academic Publishers, Dordrecht, the Netherlands, pp. 41-48, 2004.
[13] W.H. Press, S.A. Teukolsky, W.T. Vetterling, and B.P. Flannery. *Numerical Recipes in C, 2nd Edition*. Cambridge University Press, Cambridge, England, 1992.
[14] A. Dresden. *Solid Analytical Geometry and Determinants*. Dover Publications, Inc. New York, NY, U.S.A., 1964.
[15] J.A. Nelder and R. Mead. "A Simplex Method for Function Minimization". *Computer Journal*, 7: 308-313, 1965.
[16] R. Hooke and T.A. Jeeves. "Direct Search Solution of Numerical and Statistical Problems". *Journal of the ACM (JACM)*, 8(2): 212-229, 1961.